Jurnal Teknologi

Full Paper

ANATOMICAL VARIATIONS IN A FINITE ELEMENT NERVE MODEL OF THE HUMAN FOOT

Muhammad Zeeshan Ul Haqu[a,b]*, Muhammad Fahad Shamim[c], Peng Du[b], Leo K. Cheng[b]

[a]Department of Biomedical Engineering, Salim Habib University, Karachi, Pakistan
[b]Auckland Bioengineering Institute, The University of Auckland, Auckland, New Zealand
[c]Institute of Biomedical Engineering and Technology, Liaquat University of Medical and Health Science, Jamshoro, Pakistan

Article history
Received
16 January 2024
Received in revised form
1 March 2024
Accepted
1 July 2024
Published Online
20 August 2024

*Corresponding author
Muhammad.zeeshan@shu.edu.pk

Graphical abstract

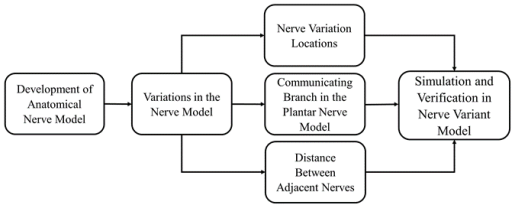

a

Abstract

The nerves in the foot offer a significant role in controlling the movement and correct loading of the foot by providing continuous feedback to the central nervous system. The health importance in the anatomical variations of nerves, such as the locations, the lengths, the communicating branches, and the distance between the adjacent nerve terminals between individuals have given prominence to anatomists as well as physiologists. A previously developed one-dimensional (1D) model of the nerve was extended to determine different anatomical variations in the nerves of the foot, as a realistic anatomical-based variant nerve model of the human foot is not available. The model was verified against experimental data from the literature for communicating branches and distances of various area of the human foot. For instance, the simulated distances of the communicating branches of the plantar nerves and medial dorsal cutaneous nerve (MDCN) division proximal to the first digital space were found to be 43.3 mm and 112.3 mm, respectively, which was in general agreement with the experimental distances of 8-56 mm and 96-116.74 mm, respectively. The developed nerve variant model provides a platform for future studies of the various geometrical and efficient concerns of neurovascular diseases such as diabetic neuropathies by determining the parameters of nerve conduction studies.

Keywords: Anatomical based variant nerve model, anatomical variations, communicating branch, central nervous system, diabetic neuropathies

1.0 INTRODUCTION

The nerves in the foot not only detect sensory inputs but also provide feedback and input to the muscles responsible for contraction and relaxation during gait [1, 2]. The nerves are affected in diabetic neuropathies and non-healing ulcers of the foot. The nerve conduction studies (NCS) can be used to asses and diagnose diabetic neuropathies [3].

The nerves in the foot consist of a mixture of unmyelinated and myelinated nerves [4]. The plantar, as well as dorsal nerves in the human foot

encompass different sensory and motor nerves that are connected with the free nerve endings in the skin [5]. The dorsal nerves of the foot comprises the superficial peroneal nerve (SPN), the sural nerve (SN), the deep peroneal nerve (DPN), and the saphenous nerve (SaN) [6, 7]. The larger SPN divides distally into the medial dorsal cutaneous nerve (MDCN), which communicates with the SaN, and splits into two digital branches. The intermediate dorsal cutaneous nerve (IDCN) incorporates with the SN and splits into two digital branches. The lateral dorsal cutaneous nerve (LDCN) develops below the lateral malleolus and covers the lateral portion of the foot and the little toe [8]. The plantar nerves consist of the tibial nerve (TN), which divides into the medial plantar nerve (MPN), the lateral plantar nerve (LPN), and the medial calcaneal nerve (MCN) [6]. The MPN comprises of cutaneous, muscular, articular, a proper digital nerve, as well as three common digital nerves and communicates with the LPN between the third and fourth common digital nerves [9, 10].

The anatomical variations of nerves in the foot play a vital role in different foot disorders. SPN compression causes pain, reduced sensation over the dorsal side and neurovascular injury [11-14]. Damage to the SN is related with the sensory loss of lateral dorsal side of the human foot [13, 15, 16], fracture of the lateral malleolus [17, 18], nerve trauma, neuroma, scar inclusion, and various ankle pathologies [8, 19, 20]. Communicating branches of the plantar nerves related clinically with Morton's neuroma [9, 21, 22], and metatarsal bone stress fracture [10, 23, 24].

The structure of the human foot nerves are complex and variable between subjects, and different imaging techniques are needed to obtain nerves structure [6]. Therefore, an anatomical-based variant nerve model of the foot provides a virtual platform to clinicians and researchers for identifying the particular nerve and its associated injury when the specific area of the foot is affected. A limited number of investigations have previously been conducted on the structural and functional consequences of the nerve model of the foot [25-27]. Previously, the normal structural plantar and dorsal nerve model was developed, followed by the nerve model of the normal intra-epidermal nerve fiber (IENF) model at different regions of the foot [28]. The second model was related with the development of structurally interrupted IENF model based on the literature based reduced IENF density (IENFD) in the various positions of the foot to simulate small fiber neuropathy [29]. In another study, a combined dorsal nerve functional nerve model was constructed using different electrophysiological nerve model for the measurement of the nerve conduction velocity in the various nerves of the foot [27]. However, none of these studies were based on the anatomical variations such as locations, communicating branches, and distance between two adjacent nerves.

The key purpose of this current work was to construct the first anatomical variant nerve model of the human foot, by expanding a previously developed anatomical nerve model [25, 26] to identify various anatomical variations in the nerve geometrical model of the foot using the identified neural anatomical structure. This study also computed length variations of the various larger nerves, and the distance between the two adjacent nerves. Furthermore, the nerve variant geometrical model was validated with the literature-based data in terms of computing the length of the foot, length of the communicating branch between MPN and LPN and the distance of the various area in the human foot. The anatomical nerve model was later on used to simulate the aforementioned anatomical variations. This variant anatomical model will provide a tool in the forthcoming studies for simulating structural and functional consequence of various neurovascular injuries such as sensory neuropathies in the foot.

2.0 METHODOLOGY

The nerve variant geometrical model was modelled using the CMISS mathematical modelling software (www.cmiss.org). The stages involved in the development of finite element variant nerve model of the human foot are as follows:

2.1 Anatomical Nerve Model

A previously developed anatomical nerve model containing various plantar and dorsal nerves was used as the starting point [25]. Briefly, the images including the MPN and LPN from the Visible Human Male (VHM) dataset [28] were manually digitized. Similarly, anatomical literature [13, 29-35] were employed and digitized in MATLAB to obtain the data clouds of the remaining plantar and dorsal nerves of the foot along with their cutaneous and muscular branches. The obtained data points were represented as node points for the development of nerve geometrical model of various plantar and dorsal nerves of the human foot in normalized local coordinated system by employing 1D cubic Hermite basis functions using iterative fitting techniques. In this work, a 1D cubic Hermite basis function was utilized to obtain the smooth nerve surfaces and reduce the number of elements required to represent complex structures.

A 3-dimensional (3D) anatomical right foot model previously developed by Fernandez et. al [36] was employed. The fitting of the foot model with the nerve geometrical model was done in such a way that different nerves of the foot could not intersect any of the muscles or bones using the manual geometrical transformation method [36]. This manual geometric transformation technique consists of geometrical scaling, translation and rotation procedures on the developed nerve model for

acquiring the realistic anatomical nerve model fitted with a 3D anatomical foot model [37]. The stages involved in fitting the nerve geometrical model with the foot anatomical model using geometrical transformation method are presented in Figure 1.

The final fitted baseline dorsal geometrical nerve model with a 3D anatomical right foot model is represented in Figure 2.

2.2 Variations in the Nerve Geometrical Model

The length, location, communicating branch and distance of the various nerves present on the dorsal and plantar side of the foot offer a significant measure of the consequent development of the nerve geometrical model. These parameters demonstrate inter-personal variations and indeed even among the two feet of the same individual, although the anatomical structure of the specific larger nerve remains relatively constant. Therefore, in this study, the different nerves were varied in the nerve geometrical model with respect to the location, communicating branch, and distance among two adjacent nerves.

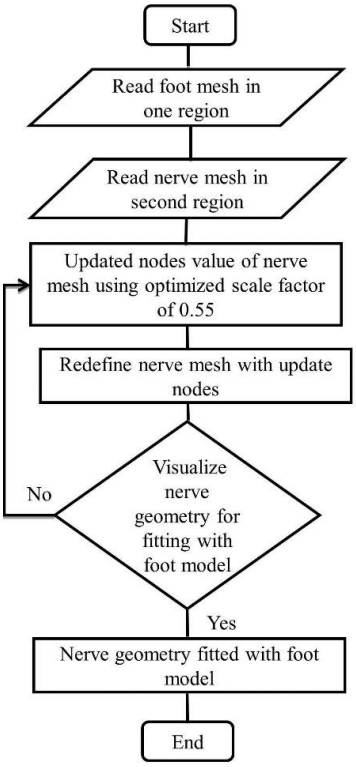

Figure 1 Flow chart representing the fitting procedure for nerve geometrical model with the foot anatomical model using geometrical transformation method

2.2.1 Nerve Location Variations

Firstly, the consequence of varying the position of distal elements from the first branch of larger dorsal MDCN was assessed while the proximal position of the remaining element of the designated larger first branch of MDCN remained in the identical location with a length of 111.4 mm. The nerves in the region between the first digital branch (big toe) up to the first branch of the MDCN (covering approximately 136 mm) were translated to 2, 4, 6 and 8 mm from its baseline position to the lateral side of the big toe as indicated in Figure 2. Both the nerve mesh of larger first branch of MDCN, one with the varying position and the other one with fixed position are re-connected using a 1D cubic Hermite Basis Function as shown in Figure 2. In addition, calculations were performed to determine the length of the various nerves present in the dorsal and plantar nerve anatomical model using Eq. (1).

$$L_T = \sum_{L_i=1}^{n} L_i \quad (1)$$

where, L_T indicates the total length of the selected nerves, and L_i represents the individual length of an element of the selected nerve present in the dorsal and plantar nerve models.

The various variable sites along with the initial site of the first MDCN branch and the initial MDCN nerve mesh are also demonstrated in Figure 2. In addition, calculations were performed to determine the length of the of MDCN, IDCN, and SN by computing the individual length of an element of the selected nerve present in the dorsal nerve model.

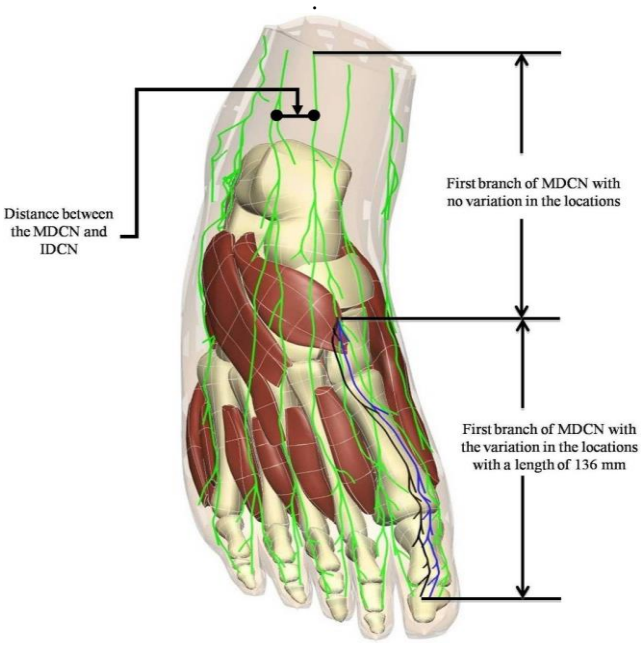

Figure 2 Representation of the normal baseline dorsal nerve geometrical model, defined by the green lines, with no variation. The variant part of the first MDCN branch (nodal transformation), defined by the blue and black lines at locations of 4 mm (blue color) and 8 mm (black color) from the normal baseline geometrical dorsal nerve model respectively. The distance between the larger MDCN and IDCN is defined by a solid black element with two node points on the left side

2.2.2 Communicating Branches

The anatomic variations in the plantar nerves communicating branches among the third as well as the fourth common digital plantar nerves are significant in the forefoot region of the foot for local injection therapy, inter-digital neuroma [9, 21, 22]. Previous investigations have studied the anatomical variations of the plantar nerves communicating branch. In Govsa *et al*. [10], the communicating branch was absent in 72% of subjects whereas, previous study reported that approximately more than 60% of subjects had the communicating branch [9]. Therefore, in this work, two different finite element nerve models with and without communicating branches in the plantar side of the foot using 1D cubic Hermite Basis functions were developed as illustrated in Figure 3.

2.2.3 Distance Between Adjacent Nerves

In this work, the distance between the two different contiguous nerves of the developed nerve geometrical model was simulated by selecting the two adjacent nerves in the proximal position. As an example, the distance between the larger MDCN and IDCN is shown in Figure 2, represented by the black color. Additionally, this study also demonstrated different anatomic landmarks of different nerves present on the plantar as well as the dorsal side of the foot as mentioned in Table 2.

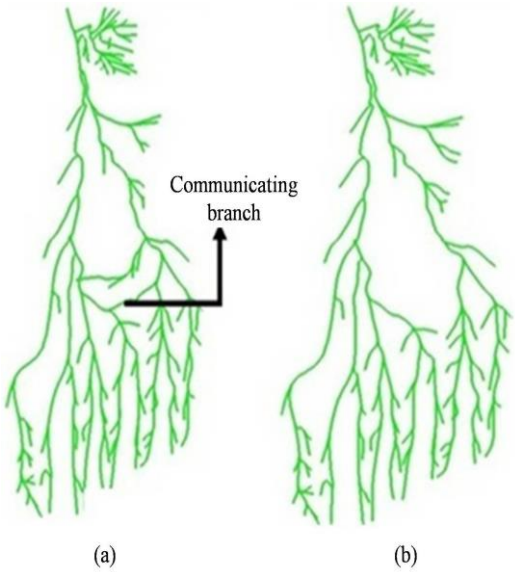

Figure 3 Plantar nerve models representing the various plantar nerves with green colour. (a) Plantar nerve model with a communicating branch. (b) Plantar nerve model with no communicating branch

3.0 RESULTS AND DISCUSSION

The total simulated length of the foot was approximately 231.1 mm. The total number of nodes and elements employed in the development of the anatomical-based geometrical dorsal and plantar nerve model of the foot were 690 and 681 respectively. These node points represented data points from the manual digitization of VHM and anatomical texts while the length of the individual element was also variable due to asymmetrical node points.

The comparison between the total length of the baseline first branch of larger MDCN (no variations) and the length of the variations in the part of the first branch of MDCN together with the other part of the larger MDCN with no variations are listed in Table 1. The location of the distal larger MDCN varied from 0 to 2 mm, 4 mm, 6 mm and 8 mm intervals respectively. This results the reduction in the length of the distal part of the MDCN and hence the total length of the first branch of larger MDCN with the variations in the location was also reduced whereas the length of the larger MDCN with no variation in the location remains the same.

Table 1 Comparison between the total length of larger MDCN with the length of the variable MDCN and length of the fixed MDCN with the variations recorded at 0, 2, 4, 6, and 8 mm.

Variations in the location (mm)	Total length of MDCN (mm)	Length of the variable MDCN (mm)	Length of the fixed MDCN (mm)
0	248.3	136.9	111.4
2	247.3	135.9	111.4
4	246.8	135.4	111.4
6	246.7	135.3	111.4
8	246.6	135.2	111.4

Additionally, the length of the different selected larger nerves in the dorsal and plantar nerve model along with their digital and inter-digital branches were also simulated and are presented in Table 2. The lengths of the various dorsal as well as plantar nerves along with their digital nerves were calculated using Eq. (1) at a different area of the selected nerves as listed in Table 2. For instance, the simulated total length of the MPN and LPN (including their superficial and proper digital branch of great toe) were 221.6 mm and 215.9 mm respectively (Table 2) respectively. Table 2 showed that the simulated length of MDCN, IDCN and SN are 65.7 mm, 67.2 mm and 262. 8 mm as compared to 81 mm, 55 mm, and 145 mm [38, 39] respectively. Unfortunately, we could not find the mean literature-based length of various plantar and dorsal nerves along with their cutaneous and muscular branches as generally the length of the nerves is not considered for the examination of various neurodegenerative disorders.

Table 2 Simulation of length variations in different larger nerves of dorsal and plantar nerve model

Nerves of the foot	Length (mm)
MDCN	65.7
First digital branch (great toe)	182.5
Second digital branch (contiguous side of second and third toes)	111
IDCN	67.2
First common digital nerves of IDCN	116.6
First proper digital nerves of IDCN (third toe)	59.2
Second proper digital nerves of IDCN (fourth toe)	48.1
	115.9
Second common digital nerves of IDCN	47.9
First proper digital nerves of IDCN (fourth toe)	42.5
Second proper digital nerves of IDCN (fifth toe)	
SN	262.8
SaN	228.4
DPN	163.8
Proper digital branch of DPN to the first toe	29.2
Proper digital branch of DPN to the second toe	60.2
Tibial nerve (TN	64.5
Superficial branch of MPN	96.7
Proper digital nerves of great toe	124.9
First common digital nerves of MPN	60.2
First proper digital nerves of MPN	71.9
Second proper digital nerves of MPN	71.9
Second common digital nerves of MPN	52.1
Second proper digital nerves of MPN	74.9
Third proper digital nerves of MPN	63.1
Third common digital nerves of MPN	31.6
Third proper digital nerves of MPN	69.8
Fourth proper digital nerves of MPN	64.4
Superficial branch of LPN	130.1
Proper digital branch of little toe	85.8
Common plantar digital nerves of LPN	31.6
Fourth proper digital nerves of LPN	64.3
Fifth proper digital nerves of LPN	61.5

The distance between two adjacent nerves along with branches in the dorsal and plantar region of the nerve geometrical model is presented in Table 3. As an example, the distance variation between the first-first toe nerve branches of the dorsal side was 21.5 mm as compared to 17.3 mm in the first-second toe nerve branches of the same dorsal side (Table 3). The distance between the first to first toe nerve branches of the dorsal region was 21.5 mm in contrast to 15.5 mm of the plantar region. Results from our larger MDCN model variation simulation studies showed that the anatomical structure of the MDCN remains the same, even when the portion of the first branch of MDCN varied (Figure 2).

The location variations can be useful in defining the nerve conduction velocity (NCV) of the variant nerve structure. There had been variations in the length of various larger nerves along with their sub-branches locating in and the dorsal part of the foot observed (Table 3). These variations in the plantar nerve length suggested that the length of the individual larger nerves in the dorsal and plantar side were dependent on the subject demographic data.

There was a significant variation observed in the various adjacent nerves and their branches in the proximal region of the dorsal as well as plantar nerve model of the foot (Table 3). The distance between the different nerve branches in the toes of the dorsal as well as plantar region of the foot was also calculated and found a less distance variation between the nerve branches in the adjacent toes in the same region or even between the same toes in the dorsal as well as plantar region nerve branches of the foot.

Table 3 Distance between the two adjacent nerves in the different sections of the anatomical nerve variant model

Dorsal Area of the foot	Distance (mm)	Plantar Area of the foot	Distance (mm)
SN to IDCN	40.1	LPN to MPN	39.2
IDCN to MDCN	14.6	Distal length to communicating branch (CB)	13.1
MDCN to DPN	17.8	CB	28.3
DPN to SaN	18.9	CB direct (LPN to MPN)	31.1
First to the second branch of IDCN	8.5		
First to the second branch of MDCN	10.9		
First to the first toe	21.5	First to the first toe	15.5
First to the second toe	17.3	First to the second toe	20.1
Second to the third toe	18.4	Second to the third toe	16.8
Third to the fourth toe	16.2	Third to the fourth toe	14.6
Fourth to the fifth toe	20.8	Fourth to the fifth toe	17.5

Simulation studies were carried out to verify different anatomical landmarks and regions for different dorsal as well as plantar nerves in the human foot with respect to the experimental based data over the same anatomical sites and regions of the foot. Table 3 lists the validation of the distance between the different regions of the foot with the literature-based distance over the same location. For example, the simulated distance between the tip of lateral malleolus to SN was 17.8 mm, and it was comparable to the experimental distance over the same region (Table 3).

In addition, different anatomical landmarks and regions of the human foot were also verified with the experimental based on the same locations (Table 4). For instance, the simulated length of the foot was 231.1 mm as compared to literature-based mean foot length 238 mm [9]. The simulated length of the communicating branch between MPN and LPN was found inside the literature-based communicating

branch length [10]. In addition, the simulated distance between medial to lateral malleolus was found 'in between the literature-based length of the same region [41]. The simulated distance of larger MDCN into three sub-branches from the first digital space was 112.3 mm in contrast to Canovas *et al*. [41] and Ikiz, and Ucerler [39] and the distance between the first branch point of MDCN and intra-malleolar was consistent with the previous study [40]. Similarly, the simulated distance of larger IDCN dissection to fourth interdigital space and branching point of IDCN was similar to the previous studies [40, 42].

Table 3 Verification of the distance of the various area of the foot from a nerve geometrical model with the literature-based distance calculated using the flexible ruler from the human cadavers' feet with their reference

Area of the foot	Simulation based length (mm)	Literature based length (mm)	References
Medial to lateral malleolus	106	102 – 11	Woo *et al*. [19]
MDCN to medial malleolus	41.1	> 20	Canovas *et al*. [18]
Communicating branch (CB)	43.3	8 – 56	Govsa et. al [10]
Proximal attached to the CB	47.4	30 – 55	Frank *et al*. [9]
Tip of lateral malleolus to SN	17.8	6.27 – 20.03	Ikiz *et al*. [17]
MDCN division proximal to first digital space	112.3	96-116.74	Ikiz, and Uceler [40]
First branching point of MDCN distal to intra-malleolar distance	32.71	14.64-35.72	Ikiz, and Uceler [40]
IDCN division proximal to fourth digital space	86.39	30.38-102.78	Ikiz, and Uceler [40]
First branching point of IDCN to distal intra-malleolar distance	43	22.48-83.3	Ikiz, and Uceler [40]

Since, the developed larger nerve geometrical model was based on VHM as well as various anatomical representations, which provided various anatomical variations and also verified various anatomical regions of the human foot. However, this nerve geometrical model had some minor limitations such as the fitting method was not used for fitting geometrical nerve model with the muscles and bones of the foot and the absence of experimental histological data from a single dataset. These limitations can be overcome by employing the host mesh fitting technique and adopting the patient-specific modeling technique [43]. Another avenue of research is to perform functional nerve conduction simulations of the variants to quantify the effects of changes in nerve structure on NCV in a systematic manner [27]. The following are the suggested steps for performing functional nerve study in the developed nerve variant model:

- Select the signal nerve fiber path using application of 1D nerve algorithm.
- Perform the functional nerve conduction study by implementing relevant nerve electrophysiological models and the appropriate numerical methods using Bidomain models.
- Compare the simulated nerve conduction velocity with the experimental studies for verification of the model.

4.0 CONCLUSION

The present work described the various anatomical variations, i.e., the locations, the presence of communicating branches, and the distance between the two adjacent larger nerves in the dorsal and plantar nerve model. After that, the model was verified with the experimental distance of the various area of the foot. In forthcoming studies, these anatomical variations will be implemented to compute the nerve action potentials and extracellular potentials using time variant nerve electrophysiological models for determining the functional evaluation of various neurovascular damages in the normal and diabetic neuropathic patients. The outcomes will be helpful for the clinicians to establish an electrochemical connection between the loading and sensory nerve feedback in healthy and diabetic neuropathic subjects.

Acknowledgement

This research study was supported by the New Economy Research Fund of New Zealand. The authors also acknowledge Prof. Merryn Tawhai, A/Prof. Justin Fernandez and Dr. Marc D. Jacobs at the Auckland Bioengineering Institute for providing their valuable guidance as well as support in the development of the model.

Conflicts of Interest

The author(s) declare(s) that there is no conflict of interest regarding the publication of this paper.

References

[1] Li, L., Zhang, S. and Dobson, J. 2019. The Contribution of Small and Large Sensory Afferents to Postural Control in Patients with Peripheral Neuropathy. *Journal of Sport and Health Science*. 8(3): 218-227.

[2] Sousa, A. S., Silva, A. and Tavares, J. M. R. 2012. Biomechanical and Neurophysiological Mechanisms Related to Postural Control and Efficiency of Movement: A Review. *Somatosensory & Motor Research*. 29(4): 131-143.
[3] Clayton Jr, W. and Elasy, T. A. 2009. A Review of the Pathophysiology, Classification, and Treatment of Foot Ulcers in Diabetic Patients. *Clinical Diabetes*. 27(2): 52-58.
[4] Lundborg, G. and Dahlin, L. B. 1992. The Pathophysiology of Nerve Compression. *Hand Clinics*. 8(2): 215-227.
[5] Pittenger, G. L., Ray, M., Burcus, N. I., McNulty, P., Basta, B. and Vinik, A. I. 2004. Intraepidermal Nerve Fibers are Indicators of Small-fiber Neuropathy in Both Diabetic and Nondiabetic Patients. *Diabetes Care*. 27(8): 1974-1979.
[6] De Maeseneer, M., Madani, H., Lenchik, L., Kalume Brigido, M., Shahabpour, M., Marcelis, S., De Mey, J. and Scafoglieri, A. 2015. Normal Anatomy and Compression Areas of Nerves of the Foot and Ankle: US and MR Imaging with Anatomic Correlation. *Radiographics*. 35(5): 1469-1482.
[7] Nayak, V. S., Bhat, N., Nayak, S. S. and Sumalatha, S. 2019. Anatomical Variations in the Cutaneous Innervation on the Dorsum of the Foot. *Anatomy & Cell Biology*. 52(1): 34.
[8] Nagabhooshana, S., Vollala, V. R., Rodrigues, V. and Rao, M. 2009. Anomalous Superficial Peroneal Nerve and Variant Cutaneous Innervation of the Sural Nerve on the Dorsum of the Foot: A Case Report. *Cases Journal*. 2: 1-5.
[9] P. Frank, B. Bakkum, and S. Darby. 1996. The Communicating Branch of the Lateral Plantar Nerve: A Descriptive Anatomic Study. *Clinical Anatomy*. 9(4): 237-243.
[10] Govsa, F., Bilge, O. and Ozer, M. A. 2005. Anatomical Study of the Communicating Branches between the Medial and Lateral Plantar Nerves. *Surgical and Radiologic Anatomy*. 27: 377-381.
[11] K. G., R. M., S. N., S., Koshy, S. and Rodrigues, V. 2010. Clinically Important Anatomical Variation of Cutaneous Branches of Superficial Peroneal Nerve in the Foot. *The Open Anatomy Journal*. 2(1).
[12] Apaydin, N., Basarir, K., Loukas, M., Tubbs, R. S., Uz, A. and Kinik, H. 2008. Compartmental Anatomy of the Superficial Fibular Nerve with an Emphasis on Fascial Release Operations of the Leg. *Surgical and Radiologic Anatomy*. 30: 47-52.
[13] Madhavi, C., Isaac, B., Antoniswamy, B. and Holla, S. J. 2005. Anatomical Variations of the Cutaneous Innervation Patterns of the Sural Nerve on the Dorsum of the Foot. Clinical Anatomy. *The Official Journal of the American Association of Clinical Anatomists and the British Association of Clinical Anatomists*. 18(3): 206-209.
[14] Kumar, S., Mangi, M. D., Zadow, S. and Lim, W. 2023. Nerve Entrapment Syndromes of the Lower Limb: A Pictorial Review. *Insights into Imaging*. 14(1): 166.
[15] Fracol, M. E., Dumanian, G. A., Janes, L. E., Bai, J. and Ko, J. H. 2020. Management of Sural Nerve Neuromas with Targeted Muscle Reinnervation. *Plastic and Reconstructive Surgery Global Open*. 8(1).
[16] Jackson, L. J., Serhal, M., Omar, I. M., Garg, A., Michalek, J. and Serhal, A. 2023. Sural Nerve: Imaging Anatomy and Pathology. *The British Journal of Radiology*. 96(1141): 20220336.
[17] iKiZ, Z. A. A., üÇerler, H. and Bilge, O. 2005. The Anatomic Features of the Sural Nerve with an Emphasis on Its Clinical Importance. *Foot & Ankle International*. 26(7): 560-567.
[18] Canovas, F., Bonnel, F. and Kouloumdjian, P. 1996. The Superficial Peroneal Nerve at the Foot. Organisation, Surgical Applications. *Surgical and Radiologic Anatomy: SRA*. 18(3): 241-244.
[19] Woo, S. B., Wong, T. M., Chan, W. L., Yen, C. H., Wong, W. C. and Mak, K. L. 2010. Anatomic Variations of Neurovascular Structures of the Ankle in Relation to Arthroscopic Portals: A Cadaveric Study of Chinese Subjects. *Journal of Orthopaedic Surgery*. 18(1): 71-75.
[20] Ferkel, R. D., Small, H. N. and Gittins, J. E. 2001. Complications in Foot and Ankle Arthroscopy. *Clinical Orthopaedics and Related Research (1976-2007)*. 391: 89-104.
[21] Giannini, S., Bacchini, P., Ceccarelli, F. and Vannini, F., 2004. Interdigital Neuroma: Clinical Examination and Histopathologic Results in 63 Cases Treated with Excision. *Foot & Ankle International*. 25(2): 79-84.
[22] Matthews, B. G., Thomson, C. E., McKinley, J. C., Harding, M. P. and Ware, R. S. 2021. Treatments for Morton's neuroma. *The Cochrane Database of Systematic Reviews*. 2021(7).
[23] Troy, K. L., Davis, I. S. and Tenforde, A. S. 2021. A Narrative Review of Metatarsal Bone Stress Injury in Athletic Populations: Etiology, Biomechanics, and Management. *PM&R*. 13(11): 1281-1290.
[24] Tallia, A. F. and Cardone, D. A. 2003. Diagnostic and Therapeutic Injection of the Ankle and Foot. *American Family Physician*. 68(7): 1356-1363.
[25] Ul Haque, M. Z., Du, P., Cheng, L. K. and Jacobs, M. D. 2012. An Anatomically-based Model of the Nerves in the Human Foot. *International Journal of Biomedical and Biological Engineering*. 6(9): 433-438.
[26] Ul Haque, M. Z., Du, P., Cheng, L. K. and Jacobs, M. D. 2014. An Anatomically Realistic Geometrical Model of the Intra-epidermal Nerves in the Human Foot. In *The 15th International Conference on Biomedical Engineering: ICBME 2013, 4th to 7th December 2013, Singapore*. 368-371. Springer International Publishing.
[27] Haque, M. Z. U., Du, P. and Cheng, L. K. 2022. A Combined Functional Dorsal Nerve Model of the Foot. *Mathematical Biosciences and Engineering*. 19(9): 9321-9334.
[28] Spitzer, V., Ackerman, M. J., Scherzinger, A. L. and Whitlock, D. 1996. The Visible Human Male: A Technical Report. *Journal of the American Medical Informatics Association*. 3(2): 118-130.
[29] Arakawa, T., Sekiya, S. L., Kumaki, K. and Terashima, T., 2005. Ramification Pattern of the Deep Branch of the Lateral Plantar Nerve in the Human Foot. *Annals of Anatomy-Anatomischer Anzeiger*. 187(3): 287-296.
[30] Birch, R. and Birch, R. 2011. The Peripheral Nervous System: Gross Anatomy. *Surgical Disorders of the Peripheral Nerves*.1-41.
[31] Sarrafian, S. K. and Kelikian, A. S. 2011. *Nerves. Sarrafian's Anatomy of the Foot and Ankle: Descriptivie, Topografphical, Functional*. 3ª ed. Philadelphia: Walters Kluwer Lippincott Williams & Wilkins. 381-427.
[32] Gilroy, A. M., MacPherson, B. R., Ross, L. M., Broman, J. and Josephson, A. eds. 2008. Atlas of Anatomy. 356-450. Stuttgart: Thieme.
[33] Agur, A. M. and Dalley, A. F. 2022. *Moore's Essential Clinical Anatomy*. Lippincott Williams & Wilkins.
[34] K. G., R. M., S. N., S., Koshy, S. and Rodrigues, V. 2010. Clinically Important Anatomical Variation of Cutaneous Branches of Superficial Peroneal Nerve in the Foot. *The Open Anatomy Journal*. 2(1).
[35] Standring, S. ed. 2021. *Gray's Anatomy e-book: The Anatomical Basis of Clinical Practice*. Elsevier Health Sciences.
[36] Fernandez, J., Ul Haque, M. Z., Hunter, P. J. and Mithraratne, K. 2012. Mechanics of the Foot Part 1: A Continuum Framework for Evaluating Soft Tissue Stiffening in the Pathologic Foot. *International Journal for Numerical Methods in Biomedical Engineering*. 28(10): 1056-1070.
[37] Fernandez, J. W., Mithraratne, P., Thrupp, S. F., Tawhai, M. H. and Hunter, P. J. 2004. Anatomically based Geometric Modelling of the Musculo-skeletal System and Other Organs. *Biomechanics and Modeling in Mechanobiology*. 2: 139-155.
[38] Agthong, S., Huanmanop, T., Sasivongsbhakdi, T., Ruenkhwan, K., Piyawacharapun, A. and Chentanez, V. 2008. Anatomy of the Superficial Peroneal Nerve Related to the Harvesting for Nerve Graft. *Surgical and Radiologic Anatomy*. 30: 145-148.

[39] Jeon, S. K., Paik, D. J. and Hwang, Y. I. 2017. Variations in Sural Nerve Formation Pattern and Distribution on the Dorsum of the Foot. *Clinical Anatomy*. 30(4): 525-532.
[40] Ikiz, Z. A. A. and Ucerler, H. 2006. The Distribution of the Superficial Peroneal Nerve on the Dorsum of the Foot and Its Clinical Importance in Flap Surgery. *Foot & Ankle International.* 27(6): 438-444.
[41] Woo, S. B., Wong, T. M., Chan, W. L., Yen, C. H., Wong, W. C. and Mak, K. L. 2010. Anatomic Variations of Neurovascular Structures of the Ankle in Relation to Arthroscopic Portals: A Cadaveric Study of Chinese Subjects. *Journal of Orthopaedic Surgery*. 18(1): 71-75.
[42] Ghetti, C. B., Mitchell, B. C., Shah, V. J., Onodera, K., Berger, G. K., Huang, B., Foran, I. M. and Kent, W. T. 2022. An Anatomic Study of the Lateral Dorsal Cutaneous Nerve using 3-Tesla MRI: A Comparison to Cadaveric Data with Surgical Applications. *Foot & Ankle International*. 43(5): 717-724.
[43] Oberhofer, K., Lorenzetti, S. and Mithraratne, K. 2019. Host Mesh Fitting of a Generic Musculoskeletal Model of the Lower Limbs to Subject-specific Body Surface Data: A Validation Study. *Applied Bionics and Biomechanics*. 2019.